

## Dynamics of helix deformation in a chiral smectic- $C^*$ liquid crystal: Optical experiments and modeling

Erik Kangas,\* Jian-Feng Li, and Charles Rosenblatt<sup>†</sup>

*Department of Physics, Case Western Reserve University, Cleveland, Ohio 44106-7079*

(Received 19 July 1995)

Measurements are reported for the optical response in the classical electroclinic geometry of a chiral smectic- $C^*$  liquid crystal. The sample was subjected to a weak ac electric field that was applied perpendicular to the helical axis. The response was found to be linear in field for  $E$  much smaller than the critical field for complete unwinding, and nearly independent of sample thickness, falling off approximately as  $f^{-1}$  in the frequency range  $200 < f < 20\,000$  Hz. The behavior is modeled by a time-dependent Landau-Ginzburg model in which both the local polarization and dielectric anisotropy are coupled to the electric field.

PACS number(s): 61.30.-v

Over the past few years considerable attention has been paid to both the similarities and differences between the ferroelectric (chiral Sm- $C^*$ ) liquid-crystal phase [1] and the antiferroelectric (chiral Sm- $C_A^*$ ) phase [2,3]. In both phases chiral molecules tilt by an angle  $\theta$  with respect to the smectic layer normal, such that a local polarization perpendicular to the molecule and in the plane of the layer is obtained. In the ferroelectric phase the azimuthal angle  $\varphi$  is everywhere the same, and the net polarization  $\langle P \rangle$  is therefore maximum; in the antiferroelectric phase the azimuthal orientation  $\varphi$  differs by approximately  $180^\circ$  in successive layers, and thus  $\langle P \rangle$  vanishes. One consequence of this layer-by-layer azimuthal alternation is the possibility of field- and temperature-driven ferroelectric phases in an antiferroelectric material [3–8]. (In these ferroelectric phases the number of smectic layers for which  $\varphi=0$  is different from the number of layers for which  $\varphi=180^\circ$ .) Another characteristic of materials that exhibit ferroelectricity and/or antiferroelectricity is that, owing to the absence of inversion symmetry, the azimuthal orientation  $\varphi$  in the ferroelectric phase necessarily exhibits a long-wavelength macroscopic helix perpendicular to the smectic layer planes [1,9]; for the antiferroelectric phase a pair of helices, displaced relative to each other by one smectic layer, obtains.

One objective of our ongoing investigations of chiral smectic liquid crystals is to characterize the dynamics of the field-driven ferroelectric phases and their transitions. At low fields the antiferroelectric helix pair is deformed and, for larger fields, ultimately unwound. (Analogous phenomena—the “deformed helix effect”—are also well known for both cholesteric and ferroelectric phases [1,10–20]). At still higher fields ferroelectric phase(s) may

be observed, ultimately leading to a field-induced ferroelectric phase at a sufficiently large field [3,6,21]. To better understand this sequence of events as a function of frequency we have first investigated the initial process of helix deformation in the less complex ferroelectric material. Two related goals of this study were to measure the electro-optic response of a high-quality material and to accurately model its behavior using an appropriate free energy. Although experimental results exist for one of the early ferroelectric materials [15], the data are not consistent with our modeling, perhaps due to spurious effects such as ionic motion. In this paper we report on a linear electro-optic effect associated with small electric field-induced deformations of the ferroelectric helix. We investigated the dynamics of this effect over a frequency range  $200 < f < 20\,000$  Hz, finding that the response approximately obeys a power law. Additionally, we have modeled the dynamics of this effect using a time-dependent Landau-Ginzburg model that involves couplings of both the polarization and dielectric anisotropy to the external field [22]. Very good agreement was found with the experimental results, encouraging the use of a modified form of this model in future studies of deformation of the antiferroelectric helices and transitions to ferroelectric phases.

Indium-tin-oxide-coated glass slides were spin coated with a polyimide, baked, and then rubbed unidirectionally to promote planar alignment. In order to assess the importance of the surfaces, several cells were assembled using Mylar spacers; the thicknesses were determined to be  $d=24, 49, 78,$  and  $99\ \mu\text{m}$  (all  $\pm 1\ \mu\text{m}$ ) using a high precision micrometer. The cells were filled in the isotropic phase with the liquid-crystal mixture SCE12, which was obtained from Merck and used without further purification. Excellent planar alignment was achieved on cooling from the nearly pitch-compensated cholesteric phase into the smectic- $A$  (Sm- $A$ ) phase, as determined by polarizing optical microscopy. Further cooling into the Sm- $C^*$  phase resulted in a regular array of light and dark stripes, corresponding to a uniform helical axis parallel to the rubbing direction, i.e., the  $\hat{z}$  axis. The cell was then placed into another oven, which was temperature con-

\*Present address: Department of Physics, Massachusetts Institute of Technology, Cambridge, Mass. 02139.

<sup>†</sup>Also at the Department of Macromolecular Science, Case Western Reserve University. Electronic address: cxr@po.cwru.edu

trolled to approximately 20 mK, and stabilized at 62.3 °C, approximately 4.1 °C below the Sm-A–Sm-C\* phase transition temperature  $T_{\text{Sm-A–Sm-C}^*} = 66.4$  °C. The oven was in turn placed between a pair of crossed polarizers, the first rotated by  $\Omega = 22.5^\circ$  with respect to the  $\hat{z}$  axis. Light from a He-Ne laser passed sequentially through the polarizer, the sample cell, the analyzer, and into a fast photodiode detector. This configuration corresponds to the classic “electroclinic geometry,” which is ordinarily used to measure the polar tilt angle of the director as a function of applied electric field on approaching the Sm-A–Sm-C\* transition from above [23]. The cell was driven with a sinusoidal ac voltage  $V$  at frequency  $f$ , which was ramped from 0 to 35 mV rms over 120 s. The detector signal was input simultaneously into a dc voltmeter so as to measure  $I_{\text{dc}}$ , and into a lock-in amplifier referenced to the driving voltage in order to measure  $I_{\text{ac}}$ . Since the applied field is weak,  $I_{\text{dc}}$  is effectively constant. In Fig. 1 we show a typical scan of the quantity  $I_{\text{ac}}/4I_{\text{dc}}$  vs  $V$ , where we clearly see that the component of signal at frequency  $f$  is linear in the driving voltage.

In the classic electroclinic experiment above  $T_{\text{Sm-A–Sm-C}^*}$ , the electric field  $\vec{E}$  induces a polar tilt  $\theta$  of the director, such that the director lies in a plane perpendicular to  $\vec{E}$  [24]. For sufficiently small  $\theta$ , it can be shown for our experimental geometry that the electroclinic response above  $T_{\text{Sm-A–Sm-C}^*}$  would be  $\theta = I_{\text{ac}}/4I_{\text{dc}}$  [23]. Thus in an electroclinic experiment  $d\theta/dE$  would be given by  $(1/4I_{\text{dc}})dI_{\text{ac}}/dE$ . Motivated by this expression, we obtain an analogous quantity for our measurements in the Sm-C\* phase. In Fig. 2 we show the quantity  $(1/4I_{\text{dc}})dI_{\text{ac}}/dE$ , which we define as  $d\langle\theta_{\text{eff}}\rangle/dE$ , as a function of frequency  $f$  for the sample of thickness  $d = 78$   $\mu\text{m}$ . The inset displays the same data as a log-log plot, and the solid line is a fitted model to be discussed below. The quantity  $\langle\theta_{\text{eff}}\rangle$  is clearly *not* the polar tilt angle—the polar tilt  $\theta = (11 \pm 0.5)^\circ$  everywhere in the sample at  $T_{\text{Sm-A–Sm-C}^*} - 4$  °C [25]—but instead represents an appropriate spatially averaged (denoted by  $\langle \rangle$ ) and optically averaged projection of the director in the plane of the cell. We note that if  $\theta$  is sufficiently small (which is

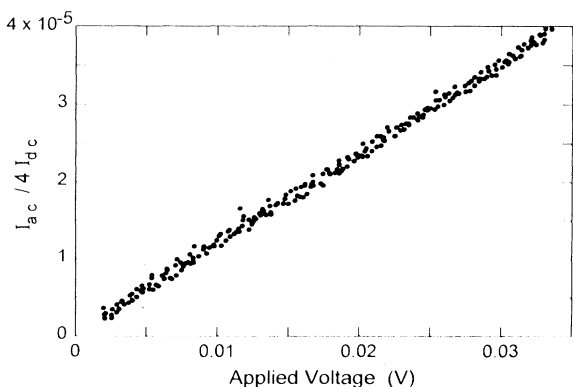


FIG. 1.  $(1/4I_{\text{dc}})dI_{\text{ac}}/dE$  vs applied rms voltage at 1.019 kHz for the 78- $\mu\text{m}$  sample.

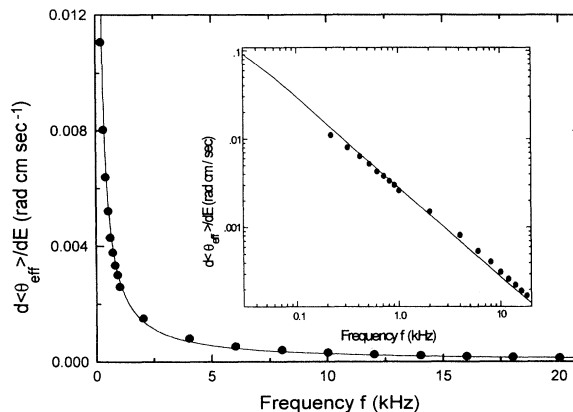


FIG. 2.  $d\langle\theta_{\text{eff}}\rangle/dE$  vs frequency for the 78- $\mu\text{m}$  cell. Solid line represents the model prediction based upon appropriate physical parameters. Inset: Log-log plot of same data.

the case here as we are only a few °C below  $T_{\text{Sm-A–Sm-C}^*}$ ), the quantity  $\theta_{\text{eff}}(z)$  can be physically associated with an optical projection of the director into the cell plane, i.e., the projection of the polar tilt. For larger  $\theta$  this interpretation breaks down. For example, if the director’s azimuthal orientation  $\varphi(z)$  were  $\pi/2$  or  $3\pi/2$ , such that the director’s tilt plane were perpendicular to the plane of the cell, then  $\theta_{\text{eff}}(z)$  would be zero. On the other hand, if  $\varphi(z)$  were 0 or  $\pi$ , such that the tilt plane lies in the plane of the cell, then  $\theta_{\text{eff}}(z)$  would be maximum, i.e.,  $\theta_{\text{eff}}(z) = 11^\circ$ .  $\langle\theta_{\text{eff}}\rangle$  is simply the spatial average of  $\theta_{\text{eff}}(z)$  over the illuminated region. Figure 3 shows a log-log plot of  $d\langle\theta_{\text{eff}}\rangle/dE$  vs frequency for the four different thickness cells. The four sets of data are in reasonable agreement over two decades of  $f$ , generally within about  $\pm 15\%$  of some average value at a given frequency. We do not believe that these differences are significant, as a given sample ( $d = 99$   $\mu\text{m}$ ) was observed to exhibit this sort of variation for several experimental runs. We there-

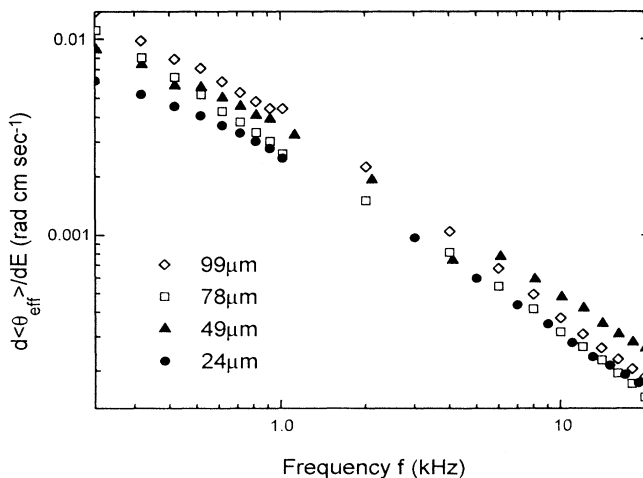


FIG. 3.  $d\langle\theta_{\text{eff}}\rangle/dE$  vs frequency for the four different cells.

fore conclude that for these thicknesses, at least, surface effects are not important.

To model the experimentally observed voltage- and frequency-dependent response, we take as our starting point the free-energy density  $F$  for a Sm-C\* liquid crystal [22]

$$F = \frac{1}{2}I \left[ \frac{\partial \varphi}{\partial t} \right]^2 + \frac{1}{2}K \left[ \frac{\partial \varphi}{\partial z} - q \right]^2 \pm PE \cos \varphi - \frac{1}{8\pi} \Delta \epsilon E^2 \sin^2 \theta \sin^2 \varphi, \quad (1)$$

where  $I$  is the moment of inertia,  $K$  is an effective twist elastic constant for molecules having a polar tilt angle  $\theta$ ,  $\Delta \epsilon$  is the dielectric anisotropy, and  $q$  the wave vector of the helical pitch. Note that the  $\pm$  refers to the stability of either the  $\varphi=0$  ( $-$ ) or the  $\varphi=180^\circ$  ( $+$ ) solution. Introducing a damping term and using a variational technique we obtain the equation of motion:

$$\eta \frac{\partial \varphi}{\partial t} = I \frac{\partial^2 \varphi}{\partial t^2} + K \frac{\partial^2 \varphi}{\partial z^2} \pm PE \sin \varphi + \frac{1}{4\pi} \Delta \epsilon E^2 \sin^2 \theta \sin \varphi \cos \varphi, \quad (2)$$

where  $\eta$  is the viscosity associated with azimuthal motion of the director. As the inertial term is important only for time scales of order  $I/\eta \sim 4 \times 10^{-14}$  s or faster, it will be dropped from the numerical computations [18]. Thus, we shall use a slightly simplified version of Eq. (2) for our analysis:

$$\eta \frac{\partial \varphi}{\partial t} = K \frac{\partial^2 \varphi}{\partial z^2} \pm PE \sin \varphi + \frac{1}{4\pi} \Delta \epsilon E^2 \sin^2 \theta \sin \varphi \cos \varphi. \quad (3)$$

For purposes of integration, we chose the following known values for the parameters at temperature  $T = T_{\text{Sm-A-Sm-C}^*} - 4^\circ\text{C}$ :  $\theta = 11^\circ$  and  $P = 14.6$  esu  $\text{cm}^{-2}$  (Ref. [25]). Additionally, we chose  $\Delta \epsilon = -1.1$  by interpolating between data in the Sm-A phase [26] and the manufacturer's specifications at  $20^\circ\text{C}$ . We also chose  $K = 10^{-8}$  dyn, a value typical of Sm-C and Sm-C\* materials tilted by a small angle [25–29]. Note that the model results turned out to be relatively insensitive to the values of  $K$  and, especially,  $\Delta \epsilon$ . Finally, we treated the viscosity  $\eta$  as an unknown, and attempted to achieve a best fit to the data.

The nonlinear partial differential equation [Eq. (3)] was solved numerically by using the ‘‘Crank-Nicholson’’ differencing scheme [30], similar to the approach of Maclennan, Handschy, and Clark [18]. This is a fully implicit scheme with second-order accuracy in time. It yields the discrete equation

$$\eta \frac{\varphi_j^{n+1} - \varphi_j^n}{\Delta t} = K \frac{\varphi_{j+1}^{n+1} - 2\varphi_j^{n+1} + \varphi_{j-1}^{n+1}}{(\Delta z)^2} - PE \sin \varphi_j^n + \frac{1}{8\pi} \Delta \epsilon E^2 \sin^2 \theta \sin \left[ 2\varphi_j^n \right], \quad (4)$$

which was solved for the next time step by inverting an  $N \times N$  tridiagonal matrix, where  $N$  is the number of discrete spatial points. The upper indices in Eq. (4)

represent the time step and the lower indices represent the spatial position.

Given our choice of sign ( $-PE \sin \varphi_j^n$ ) in Eq. (4),  $\varphi=0$  is a fixed point ( $\vec{P}$  parallel to  $\vec{E}$ ) and  $\varphi=\pi$  is metastable ( $\vec{P}$  antiparallel to  $\vec{E}$ ). Thus it is clear that, for small fluctuations of  $\varphi$  about its equilibrium, each half pitch of the liquid crystal can be considered independently. From polarized optical microscopy we determined the pitch  $2\pi/q = 14.68 \pm 0.1$   $\mu\text{m}$  for the 78- $\mu\text{m}$  sample, where it was found that the modeling results did not depend strongly on this value. (The pitches for the other samples were  $17.14 \pm 0.1$   $\mu\text{m}$  for the  $d=24$   $\mu\text{m}$  sample,  $15.14 \pm 0.1$   $\mu\text{m}$  for the  $d=49$   $\mu\text{m}$  sample, and  $14.29 \pm 0.1$   $\mu\text{m}$  for the  $d=99$   $\mu\text{m}$  sample. The increase in pitch with decreasing sample thickness is due to anchoring effects at the boundaries that tend to unwind the helix. As is the case with an electric field [31,32] the pitch increases when the helix is unwound.) We used  $N=200$  numerical points over a half pitch, corresponding to a mesh  $\Delta z = \pi/qN = 0.0367$   $\mu\text{m}$ . This yielded a very good representation of the director orientation without numerical instability. The initial condition was chosen to be  $\varphi=qz$ , corresponding to the  $E=0$  equilibrium orientation, while the ends of the half-pitch region were pinned at  $\varphi=0$  and  $\pi$ , respectively [18].

The response of the director was examined as a function of  $E$  and  $f$ . It was found that dividing the period  $\tau (= 1/2\pi f)$  of the electric field into 500 equal time steps, i.e.,  $\Delta t = \tau/500$ , inhibited numerical instability. From the discrete profile  $\varphi(z, t)$  we calculated the expected optical response  $d\langle \theta_{\text{eff}} \rangle / dE \equiv (1/4I_{\text{dc}}) dI_{\text{ac}} / dE$ . Computations starting from Maxwell's equations yield the intensity ratio  $T$  (Ref. [18])

$$T = \sin^2 \{ 2[\Omega - \tan^{-1}(\tan \theta \cos \varphi)] \} \sin^2 \left[ (n_e - n_o) \frac{\pi d}{\lambda c} \right], \quad (5)$$

where  $T$  is the ratio of the local transmitted to incident light intensity. Note that because  $\varphi = \varphi(z, t)$ ,  $T$  also varies periodically with both position and time. For calculational purposes we have used the experimental polarizer orientation  $\Omega = 22.5^\circ$ , the extraordinary refractive index  $n_e = 1.671$ , and the ordinary index  $n_o = 1.491$  (Ref. [25]). Additionally,  $c$  is the speed of light in vacuum. This formula for  $T$  neglects reflections at the air-glass interfaces and also assumes that  $n_e \approx n_o \approx n_{\text{glass}}$ , thus ignoring some of the more complicated thickness-dependent effects such as internal reflections. The spatial average  $\langle T \rangle$  was computed by averaging  $T(\varphi(z))$  over the 200 spatial points. The dc intensity  $I_{\text{dc}}$  is therefore proportional to the time average of  $\langle T \rangle$  over one period of the applied voltage, and was found to be constant in  $V$ . Likewise, the ac intensity  $I_{\text{ac}}$  is proportional to the rms amplitude of the ac component of  $\langle T \rangle$ . (Because the driving field is weak, the higher harmonics are vanishingly small, and only the component at frequency  $f$  survives.) From the calculated values  $I_{\text{ac}}$  and  $I_{\text{dc}}$  we extracted  $d\langle \theta_{\text{eff}} \rangle / dE$ .

The numerical procedure was applied for several values of  $\eta$  for the  $d=78$   $\mu\text{m}$  sample, where a best fit was

obtained for  $\eta=0.055$  P; this is shown by the solid line in Fig. 2 and the inset. We note that this value of viscosity is of the same order as the value  $\eta=0.037$  P obtained at the same reduced temperature in SCE12 for a bendlike mode [25], and is sensitive numerically to variations in the polar tilt angle  $\theta$ . Although the fit is not perfect, it is nevertheless in very good agreement both quantitatively and qualitatively with the experimental results. The small difference in apparent slopes seen in the log-log plot of Fig. 2 may come from a number of different sources, but most likely comes from small but non-negligible surface effects and approximations in the optics leading to Eq. (5). The results, both experimental and numerical, clearly show that the response of this linear electro-optic effect falls off more slowly with frequency than, for example, a Lorentzian. This is due largely to the convolution of the director dynamics [33] and optical properties of the liquid crystal [18]. Interestingly, over two decades of frequency, the optical response, both experimental and theoretical, scales approximately as  $f^{-1}$ . (The results reported in Ref. [15] deviate strongly from this behavior over the same frequency range.) Additionally, as expected the optical response scales as  $\eta^{-1}$ . Although the equations are formally valid at higher voltages—indeed, they hold even for the case of a completely unwound helix—the boundary conditions are not. At higher applied fields close to  $E_{th}$  the pitch begins to change, an effect not ac-

counted for in our simple model. Nevertheless, one could in principle use this formalism to study the optical response of a helix that is *nearly* unwound in an external field. Additionally, we note that  $\varphi$  varies in space with a soliton-lattice-like behavior at large  $E$  [22,34] in which the lattice points are pinned at the stable and metastable points, i.e., the half pitch points. For sufficiently large field these points may become unstable, propagate, and merge, yielding a net increase in pitch with  $E$ . Finally, we point out that neither the results nor the experiment requires a small polar angle  $\theta$ . Experimentally we measured an ac and a dc response, and theoretically we calculated its ratio. Only if we wish to physically associate the ratio with an effective angle  $\langle\theta_{eff}\rangle$  must  $\theta$  be small.

To summarize, we have experimentally investigated the frequency response of a linear electro-optic effect associated with the perturbation of the helical structure of a Sm-C\* liquid crystal. We have successfully modeled our results, finding that the response falls off more slowly with frequency than a simple Lorentzian line shape. This formalism can be adapted to nearly complete unwinding of the Sm-C\* phase, and can be used to study the dynamics of the antiferromagnetic double helix in external fields.

This work was supported by the National Science Foundation's Solid State Chemistry Program under Grant No. DMR-9502825.

- 
- [1] R. B. Meyer, L. Liebert, L. Strzelecki, and P. Keller, *J. Phys. (Paris) Lett.* **36**, L69 (1975).
- [2] A. D. L. Chandani, T. Hagiwara, Y. Suzuki, Y. Ouchi, H. Takezoe, and A. Fukuda, *Jpn. J. Appl. Phys.* **27**, L729 (1988).
- [3] A. D. L. Chandani, Y. Ouchi, H. Takezoe, A. Fukuda, K. Terashima, K. Furukawa, and A. Kishi, *Jpn. J. Appl. Phys.* **28**, L1261 (1989).
- [4] M. Fukui, H. Orihara, Y. Yamada, N. Yamamoto, and Y. Ishibashi, *Jpn. J. Appl. Phys.* **28**, L849 (1989).
- [5] E. Gorecka, A. D. L. Chandani, Y. Ouchi, H. Takezoe, and A. Fukuda, *Jpn. J. Appl. Phys.* **29**, 131 (1990).
- [6] K. Hiraoka, Y. Takanishi, K. Skarp, H. Takezoe, and A. Fukuda, *Jpn. J. Appl. Phys.* **30**, L1819 (1991).
- [7] T. Isozaki, T. Fujikawa, H. Takezoe, A. Fukuda, T. Hagiwara, Y. Suzuki, and I. Kawamura, *Phys. Rev. B* **48**, 13 439 (1993).
- [8] Ch. Bahr, D. Fliegner, C. J. Booth, and J. W. Goodby, *Phys. Rev. E* **51**, R3823 (1995).
- [9] See, for example, *Ferroelectric Liquid Crystals*, edited by J. W. Goodby, R. Blinc, N. A. Clark, S. T. Lagerwall, M. A. Osipov, S. A. Pikin, T. Sakurai, K. Yoshino, and B. Zeks (Gordon and Breach, Philadelphia, 1991).
- [10] E. Sackmann, S. Meiboom, and L. C. Snyder, *J. Am. Chem. Soc.* **89**, 5982 (1967).
- [11] J. Wysocki, J. Adams, and W. Haas, *Phys. Rev. Lett.* **20**, 1025 (1968); **21**, 1791 (1968).
- [12] R. B. Meyer, *Appl. Phys. Lett.* **14**, 208 (1968).
- [13] P. G. DeGennes, *Solid State Commun.* **6**, 163 (1968).
- [14] W. Kuszynski, *Ber. Bunsenges Phys. Chem.* **85**, 234 (1981).
- [15] L. A. Beresnev, V. A. Baikalov, and L. M. Blinov, *Ferroelectrics* **58**, 245 (1984).
- [16] B. I. Ostrovskii, A. Z. Rabinovich, and V. G. Chigrinov, in *Advances in Liquid Crystals Research and Applications*, edited by L. Bata (Pergamon, Budapest, 1981).
- [17] D. S. Parmar, K. K. Raina, and J. Shankar, *Mol. Cryst. Liq. Cryst.* **103**, 77 (1983).
- [18] J. E. MacLennan, M. A. Handschy, and N. A. Clark, *Phys. Rev. A* **34**, 3554 (1986).
- [19] B. I. Ostrovskii, A. Z. Rabinovich, A. S. Sonin, and B. A. Strukov, *Zh. Eksp. Teor. Fiz.* **74**, 1748 (1978) [*Sov. Phys. JETP* **47**, 912 (1978)].
- [20] B. I. Ostrovskii, S. A. Pikin, and V. G. Chigrinov, *Zh. Eksp. Teor. Fiz.* **77**, 1615 (1979) [*Sov. Phys. JETP* **50**, 811 (1979)].
- [21] A. Fukuda, Y. Takanishi, T. Isozaki, K. Ishikawa, and H. Takezoe, *J. Mater. Chem.* **4**, 997 (1994).
- [22] P. E. Cladis, H. R. Brand, and P. L. Finn, *Phys. Rev. A* **28**, 512 (1983).
- [23] G. Andersson, I. Dahl, P. Keller, W. Kuczynski, S. T. Lagerwall, K. Skarp, and B. Stebler, *Appl. Phys. Lett.* **51**, 640 (1987).
- [24] S. Garoff and R. B. Meyer, *Phys. Rev. Lett.* **38**, 848 (1977).
- [25] M. H. Lu, K. A. Crandall, and C. Rosenblatt, *Phys. Rev. Lett.* **68**, 3575 (1992).
- [26] Z. Li, G. A. DiLisi, R. G. Petschek, and C. Rosenblatt, *Phys. Rev. A* **41**, 1997 (1990).
- [27] C. Rosenblatt, R. B. Meyer, R. Pindak, and N. A. Clark, *Phys. Rev. A* **21**, 140 (1980).
- [28] M. Kawaida and T. Akahane, *Jpn. J. Appl. Phys.* **29**, 340 (1990).

- [29] T. Akahane and M. Nakagawa, *Jpn. J. Appl. Phys.* **25**, L661 (1986).
- [30] W. H. Press, S. A. Teukolsky, W. T. Vetterling, and B. P. Flannery, *Numerical Recipes in C* (Cambridge University Press, New York, 1992).
- [31] S. A. Rozanski, *Phys. Status Solidi (a)* **79**, 309 (1983).
- [32] P. G. DeGennes and J. Prost, *The Physics of Liquid Crystals* (Clarendon, Oxford, 1993).
- [33] I. Musevic, R. Blinc, B. Zeks, C. Filipic, M. Copic, A. Seppen, P. Wyder, and A. Levyanuk, *Phys. Rev. Lett.* **60**, 1530 (1988).
- [34] B. Zeks and M. Cepic, *Liq. Cryst.* **14**, 449 (1993).